BIBECHANA
Vol. 23, No. 1, January 2026, 68-76

ISSN 2091-0762 (Print), 2382-5340 (Online)
Journal homepage: http://nepjol.info/index.php/BIBECHANA
Publisher:Dept. of Phys., Mahendra Morang A. M. Campus (Tribhuvan University)Biratnagar

GNSS-RO investigation of tropopause dynamics surrounding the geomagnetic storm of 10–13 May 2024

Tulashi Gautam [1,2], Madhu Sudan Paudel [1,2,*], Basu Dev Ghimire [3], Narayan Prasad Chapagain [4],

[1]*Department of Physics, Tri-Chandra Multiple Campus, Tribhuvan University, Nepal*
[2]*Central Department of Physics, Tribhuvan University, Nepal*
[3]*Department of Physics, St. Xavier's College, Tribhuvan University, Nepal*
[4]*Department of Physics, Amrit Campus, Tribhuvan University, Nepal*
[*]Corresponding author. Email: mspaudel27@gmail.com

Abstract

The tropopause is the transitional layer between the troposphere and stratosphere, which has significance in the weather monitoring and forecasting, aviation technology, and other various fields. GNSS-RO is a method that is widely used to study and understand the atmospheric properties and the phenomena related to it. In this study, the atmospheric data from the Constellation Observing System for Meteorology Ionosphere and Climate – 2 (COSMIC-2) mission are used to understand the impact of geomagnetic storm from 10-13 May 2024 on the tropopause parameters. The tropopause height (TRH) and tropopause temperature (TRT) is calculated using the World Meteorological Organization 1957 (WMO 1957) criteria during, before and after the geomagnetic storm time as well as on the same days in previous years. The result obtained is compared to each other. During the geomagnetic storm time, global variation of TRH with longitude shows almost constant nature in tropical region (0° to ∼23° latitude) and higher-latitude (> 35°) region but sharp changes is observed in sub-tropical region (∼23° to ∼35° latitude). The increase in TRH can be seen in tropical region when compared to prior years, which might be due to global warming and global increase in temperature in May 2024. A comparison of TRH and TRT before, during and after geomagnetic storm is performed using paired t-test. A significant change in TRH and TRT can be observed in tropical and higher latitude (> 35°) during and after the geomagnetic storm. Which supports the physical mechanism of coupling between the ionosphere and upper troposphere during geomagnetic storm.

Keywords: GNSS-RO, Tropopause dynamics, WMO, Tropopause height, Tropopause temperature, Geomagnetic Storm, 10-13 May 2024.

Article information
Manuscript received: March 17, 2025; Revised: September 13, 2025; Accepted: November 7, 2025
DOI https://doi.org/10.3126/bibechana.v23i1.76695

1 Introduction

The atmosphere is divided into five different layers, from lower towards higher altitude: the troposphere, stratosphere, mesosphere, thermosphere and exosphere. The tropopause is the boundary layer between the troposphere and the stratosphere, which is characterized by the rate of temperature change with altitude, also known as the lapse rate (LR) [1, 2]. Tropopause is not a fixed boundary; its variation is referred as tropopause dynamics. A number of different factors influences tropopause dynamics, like; atmospheric weather events, large-scale circulation patterns, extreme weather conditions, etc., [3]. Space weather phenomenon like solar flare, geomagnetic storm, etc., also have the influence on middle atmosphere and troposphere [4, 5]. The geomagnetic storm is a temporary disturbance of the Earth's magnetic field, which originates from solar wind disturbances. This can either be in the form of Coronal Mass Ejections (CME) or Solar Flares (SF). In SF, the energy is released in the form of photons and charged particles. The strong magnetic fields of the CME cause the most powerful storms when it collides with the magnetosphere of the Earth [6, 7]. These storms can have large effects on communication networks, satellite operations, and even power grids. Global Navigation Satellite System-Radio Occultation (GNSS-RO) is a method that is widely used to study and understand the atmospheric properties and various phenomena.

Occultation is the condition in which the two-communicating link is not in a straight line of sight and blocked by some object. In case of GNSS-RO the Earth's atmosphere blocks the direct straight communication link between the two satellites. The signal from the transmitting satellite still reaches the receiving satellite due to the bending by the atmosphere of the Earth. By calculating the bending angle profile, the properties of various layers of atmosphere can be studied with great vertical resolution [8, 9].

In this work, we have studied the nature of global TRH and TRT during the geomagnetic storm 10-13 May 2024. The common geomagnetic storms Dst index lies below -200nT while this geomagnetic storm of May 2024 had the Dst index falls below -400nT marking it one of the strong superstorms experienced in recent years [10]. Also, to know the effect of geomagnetic storm on tropopause parameter, the result is compared with the days before and after geomagnetic storm as well as in the same days in previous years.

2 Methodology

2.1 Sources of Data

The major data used in this study are sourced from the website of Taiwan Space Agency's (https://tacc.cwa.gov.tw/data-service/), which provides GNSS-RO data from the COSMIC-2 mission [9]. This data is publicly accessible and offers a variety of datasets pertinent to the ionosphere, atmosphere, climate, and related fields. The atmospheric profiles data, labeled as 'atmPrf', are retrieved using Radio Occultation (RO) techniques. These profiles primarily include the dry component of the neutral atmosphere, which is critical for the understanding atmospheric composition and dynamics. This data type is particularly useful for studying atmospheric pressure, temperature, and humidity at various altitudes. The information of the geomagnetic parameters, such as; Kp index, Dst index, are taken from the NASA's Omni Web Data Explorer (https://omniweb.gsfc.nasa.gov/). The information of the geomagnetic quiet and disturb days is obtained from website of International Service of Geomagnetic Indices (https://isgi.unistra.fr/).

2.2 Atmospheric Parameters from GNSS-RO

GNSS RO technique is used to extract atmospheric parameters from signals received from GNSS satellites. The radio waves from GNSS satellites that passes through Earth's atmosphere are collected by low earth orbit (LEO) satellites equipped with the GNSS receivers. The variations in temperature, humidity, pressure and density of the various layers of the Earth's atmosphere cause the GNSS signals to be refracted as they pass through it. The excess phase of the refracted GNSS signals, measured by LEO satellite, provides information about the atmospheric delay of the signal on passing through the different layers of atmosphere [11].

The bending angle of the ray as it passes through the atmosphere and reaches the LEO satellite is given as [11]:

$$\alpha(a) = \int_a^b \frac{dn(\mu)}{\sqrt{x^2 - a^2}} \tag{1}$$

Here, 'a' is the impact parameter and 'μ' is the refractive index. The refractive index profile of the atmosphere can be obtained by the Abel transformation of the equation (1), which is given as [12,13]:

$$\mu = exp\left[\frac{1}{\pi}\int_x^\infty \frac{\alpha(a)}{\sqrt{(a^2 - x^2)}} da\right] \tag{2}$$

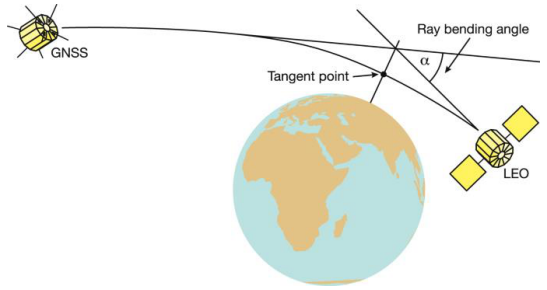

Figure 1: The bending of GNSS signal as it passes through the atmosphere and reaches the LEO satellite [12].

The relation that relates the reflectivity (N) to the refractive index profile (μ) is:

$$N = (\mu - 1) \times 10^6 \tag{3}$$

The reflectivity depends on the dry air pressure, temperature, and water vapor pressure within the neutral atmosphere, which is expressed as:

$$N = K_1 \frac{P_d(z)}{T(z)} + K_2 \frac{e(z)}{T(z)} + K_3 \frac{e(z)}{T^2(z)} \tag{4}$$

The first term represents the contribution due to dry air reflectivity, which is significant up to an altitude of 60 km and the second term is for the wet component, which is relevant up to 8 km to 10 km altitude [13, 14].

To include the ionospheric contribution another term is added which gives the following complete equation:

$$N = K_1 \frac{P_d(z)}{T(z)} + K_2 \frac{e(z)}{T(z)} + K_3 \frac{e(z)}{T^2(z)} + K_4 \frac{N_c}{f^2} \tag{5}$$

The values of constant in the above equations are as

$K_1 = 77.67$ Kmb^{-1}, $K_2 = 70.71$ Kmb^{-1}, $K_3 = 3.734 \times 10^5$ Kmb^{-1} and $K_4 = 40.3 \times 10^6$ Kmb^{-1} [14].

2.3 Tropopause Estimation: World Meteorological Organization 1957 (WMO 1957) Method

The general convention of World Meteorological Organization held on 1957 (WMO 1957) uses the concept of LR to define the tropopause [15]. LR can be defined as rate of drop in the temperature with respect to the altitude on moving up in the atmosphere. If T denotes the temperature and z denotes the altitude then:

$$LR = -\frac{dT}{dz} \tag{6}$$

The -ve sign indicates that the temperature decreases as the altitude increases. The WMO 1957 defines the tropopause using the two conditions of the LR, which are; (i) lowest altitude point at which the lapse rate drops below $2°C$/km and, (ii) the average LR should not be greater than $2°C$/km for the next 2km. The first condition helps in identifying the point from where the atmospheric transition from troposphere to stratosphere starts and the second condition ensures that the identified transition layer is not just a temporary layer and is an actual tropopause [15].

The details of the python program for the estimation of LR and tropopause is given below.

For the estimation of LR we require datasets of altitude, temperature, latitude and longitude. The following python code is used to estimate LR.

```
def LR_estimate(altitudes,temp,latitude,longitude):
    LR = [ ]
    h_data = [ ]
    t_data = [ ]
    lat = [ ]
    lon = [ ]
    for i in range(1, len(altitudes)):
        altitude_diff = altitudes[i] - altitudes[i-1]
        temperature_diff = temp[i] - temp[i-1]
        lapse_rate = -temperature_diff / altitude_diff
        lat.append(latitude[i])
        lon.append(longitude[i])
        LR.append(lapse_rate)
        h_data.append(altitudes[i])
        t_data.append(temp[i])
    return [LR, h_data, t_data, lat, lon]
```

These five variables LR, h−data, t−data, lat, lon are used to estimate the TRH and TRT alog with their respective latitude and longitude using following python code.

```
def estimate_trop(h_data,t_data,LR,latitude,longitude):
    tropopause_level = None
    lat_twh = None
    lon_twh = None
    steps = 200  # for 2km, there are 200 steps of 10m
    num_levels = len(LR)
    for i in range(num_levels):
    if LR[i] <= 2:
    within_2km = LR[max(i,0):min(i+steps, num_levels-1)]
    variation = np.mean(within_2km)
    if variation <= 2:
          trh = h_data[i]
          trt = t_data[i]
          lat_tropo = latitude[i]
          lon_tropo = longitude[i]
          break
    return [trh, trt, lat_tropo, lon_tropo]
```

2.4 Cubic Spline Interpolation: CSI

Cubic spline interpolation (CSI) is used to improve the vertical resolution of atmospheric data obtained from COSMIC-2 satellite. While the COSMIC-2 satellite data has a good vertical resolution of approximately 20m, further interpolation is performed to achieve even finer vertical resolution. This further interpolation to make the finer vertical resolution (∼10m) make sure that the continuity and stability of each atmospheric profile is smooth which helps in the precise determination of the tropopause parameter (TRT and TRH). CSI takes two-dimensional variables and uses them to create a smooth curve that passes through all the data points. CSI is advantageous because it minimizes the overall curvature of the interpolating function, leading to a smooth and natural fit that avoids oscillations [16]. In this work, we have to interpolate for four variables, which are; altitude, temperature, latitude and longitude. But CSI takes only 2 variables at a time. This can be done by interpolating multiple times for temperature, latitude and longitude by taking fixed array of the altitude, similar to the Paudel et. al, (2024) [17].

2.5 Data Pre-processing

The data obtained from the COSMIC-2 has more than 5000 atmospheric profiles per day. Not all the atmospheric profiles are good as several factors influence them. In order to get better result, we must process the data to remove the irregular and bad profiles that may introduces error in the calculation. In order to sort out the bad profiles we employ certain conditions. A complete GNSS-RO atmospheric profile must cover from the surface to the 60 km. Therefore, those profiles starting above the 10km altitude and ends below 40km are removed following Paudel et. al, (2024) [17]. This filtering criteria drastically improved the vertical profile of temperature. The study on global tropopause variation by Seidel et al. (2001) [18], the tropical tropopause by Randel et al. (2003) [19] and Fueglistaler et al. (2009) [20] found the typical range for the tropopause temperature to lie in between approximately –100°C to –40°C. The values of temperature which are colder than -100°C and warmer than –40°C are physically implausible and are likely due to the misidentified or false tropospheric inversion rather than the true tropospheric condition. Hence, the atmospheric profiles with the tropopause temperature lying outside of that range were filtered during the preprocessing.

The height of the TRH also varies with latitude (φ), the minimum cutoff value of TRH is given by [21]:

$$h_{cutoff} = 7.5 + 2.5\cos(\varphi) \quad (7)$$

The lower limit of the interpolated array of altitude is set either equal or greater than h_{cutoff} so that the estimated TRH is more than the cutoff value at given latitude.

In figure 2, the left figure shows sample of all the atmospheric profiles and the right figure shows the atmospheric profiles after applying all pre-processing criterion on that sample. After applying pre-processing criterion, most of the atmospheric profiles having irregular shape in troposphere are removed.

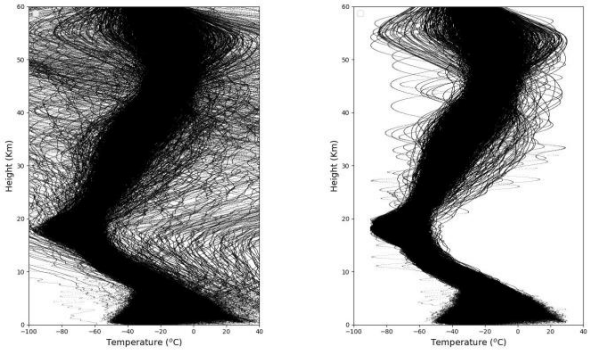

Figure 2: Atmospheric profiles before and after applying pre-processing criterion.

2.6 Region and Time-Period of Interest

The region of interest of our study is global coverage of the COSMIC-2 satellite constellation from 45°S to 45°N in latitude and 180°W to 180°E in longitude [9]. This wide geographic range enables for then in-depth analysis of the global variation in the tropopause caused by several factors. The time-period of the interest is 10-13 May 2024, at which prominent geomagnetic storm had hit on the Earth [10]. The figures 3 and 4 are the evidence of geomagnetic storm in this time. Between 10-13 May 2024, the disturb storm time (Dst) index is less than -400 nT, Kp index is more than 8 and magnetic field ∼70 nT can be seen. The GNSS-RO data from COSMIC-2 at time-period of interest can provide insight into the influence of geomagnetic storm to change global TRH and TRT. These changes are compared to the days before (26-19 April and 4-7 May) and after the storm (17-20 May and 26-29 May). In addition to 2024 events, the data of the same period, 10-13 May, from 2020 to 2023 is also used to identify patterns and anomalies in the global TRH and TRT, which may be caused due to geomagnetic storm.

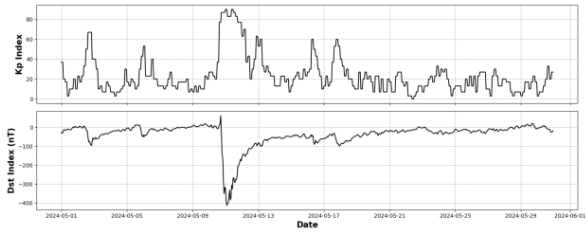

Figure 3: Kp and Dst index in the month of May, 2024

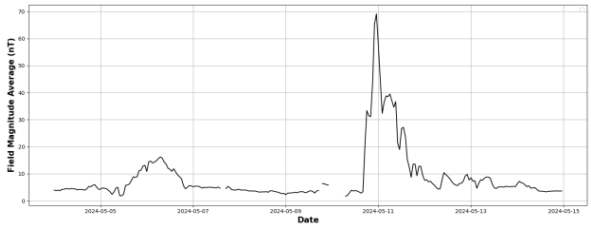

Figure 4: Average field magnitude in May, 2024. A sharp peak on 11 May, can be seen as the indication of geomagnetic storm.

2.7 Paired t-Test

The paired t-test is used as a statistical tool to test the statistical significance whether there was any significant difference in TRH and TRT before, during and after the geomagnetic storm. Before applying the paired t-test the normality of the data was verified using the Shapiro–Wilk test. All comparisons showed that the p-values were greater than 0.05 which confirmed that the data were approximately normally distributed and that the t-test was suitable for testing statistical significance. For this the data were made as a pair: one before and during storm and the other during and after the storm and the pairs were subjected to paired t-test. The t-statistics for paired t-test is given as [22];

$$t = \frac{\bar{d}}{\sigma_d/\sqrt{n}} \tag{8}$$

where, $\bar{d}$ and σ_d are the mean and standard deviation of difference between two set of data and n is sample size.

We have also estimated p-value to find the probability of getting t-statistics as extreme value than observed value. The p-value for the two tailed t-test is given by;

$$p = 2 \times P[T > (t_{calc})] \tag{9}$$

where, T follows the t-distribution with degree of freedom (n-1).

3 Results and Discussion

3.1 Variation of Global TRH and TRT

The global TRH and TRT in the active storm days, 10-13 May 2024, is shown in figure 5. In this figure, latitude is divided into 36 bins, so that each bin represents the 2.5° latitude. The box plot of each bin can be seen along with respective mean, median, standard deviation(SD) and extreme values whiskers (EVW). In the tropical region, up to ∼23°, in both northern and southern hemisphere, the value of TRH is seen almost constant with small SD.

In sub-tropical region, ∼23° to ∼35° latitude, TRH values decrease sharply with large SD and EVW. Beyond sub-tropical region, > 35° latitude, TRH becomes more or less constant, but it has slightly higher value in northern hemisphere. The TRT variation shows concave shape from 0° to 30° latitude. Beyond 35° longitude it became more or less constant, but its value is slightly less in northern hemisphere. This may be due to the inclination of the northern hemisphere of Earth towards the Sun in this time.

The variation of the global TRH and TRT in geomagnetic quietest period from 26-29 May 2024 is shown in figure 6. The variation trend of the TRT and TRH looks similar in tropical region to that of 10-13 May but there are few differences in sub-tropical region and beyond, which can be seen in figure 8. Comparison of the global TRH and TRT from 10-13 May, from 2020 to 2024. In tropical region, TRH is found to be increased in 2024 as compared to the prior year but the condition is different in sub-tropical and high latitude region.

Moreover, beyond sub-tropical region (> 35°), the TRH behavior is different in southern and northern hemisphere, maximum in northern and minimum in southern hemisphere in 2024 compared to previous year. The behavior of the global TRT is also different at tropical, sub-tropical and beyond sub-tropical region in 2024 and other years.

3.2 Comparison of the Global TRH and TRT Before, During and After Geomagnetic Storm

The comparison of the global TRH and TRT before and after the geomagnetic storm in 2024 can be seen in figure 8. The days from 26-29 April to 26-29 May are taken into the consideration for the comparison. This process helps to extract the anomalies in TRH and TRT due to seasonal effect. The visualization of the graph shows that there is no any notable difference in TRH and TRT between geomagnetic storm time and other time-period in tropical region but some difference can be observed in sub-tropical and higher latitude. We have also

compared TRH and TRT separately between geomagnetic storm days, from 10-13 May, with quite days, from 26-29 May, shown in figure 9.

For the quantitative analysis, we performed the two tailed paired t-test. The data of TRH and TRT before the storm from 4-7 May and after the storm from 26-29 May is compared with storm time 10-13 May. The result is presented in Table 1. It is observed that there is no any significant difference between TRH and TRT before and during the geomagnetic storm.

But the result obtained for during and after the storm time is different. The result indicates that TRH and TRT do not differ significantly in the subtropical region (23°–35°); however, both parameters show significant variations within the tropical region (0°–23°). Beyond subtropical region (>35°) significant difference is observed for only TRT.

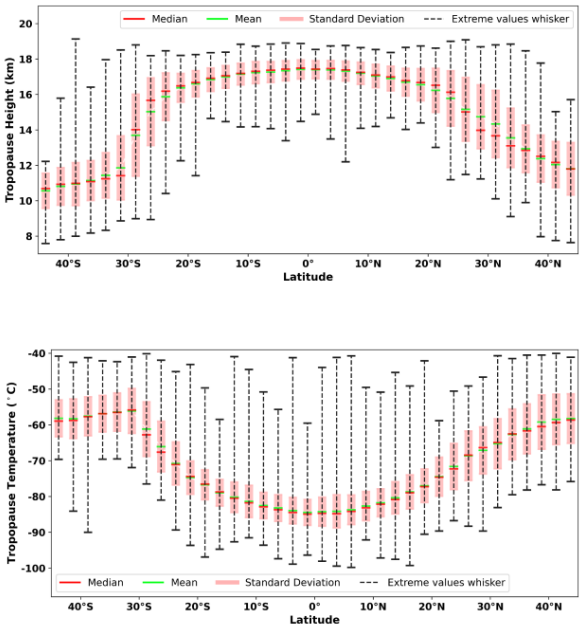

Figure 6: Global TRH and TRT variation along latitude, showing mean, median, standard deviation and extreme values in 26-29 May 2024.

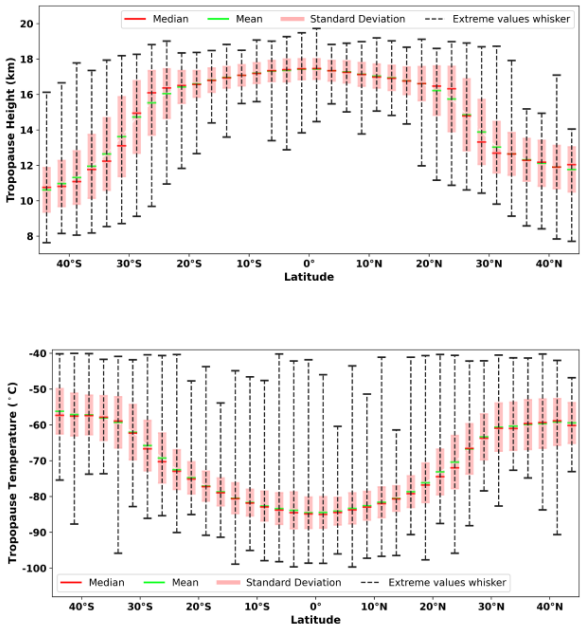

Figure 5: Global latitudinal variation of TRH and TRT showing mean, median, standard deviation and extreme values in 10-13 May 2024.

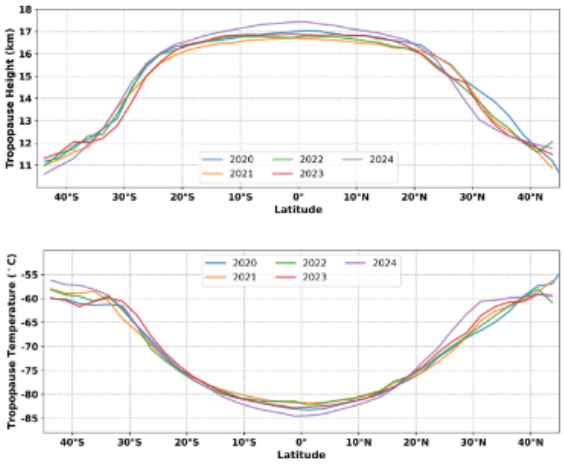

Figure 7: Comparison of the global TRH and TRT in 10-13 May from 2020 to 2024.

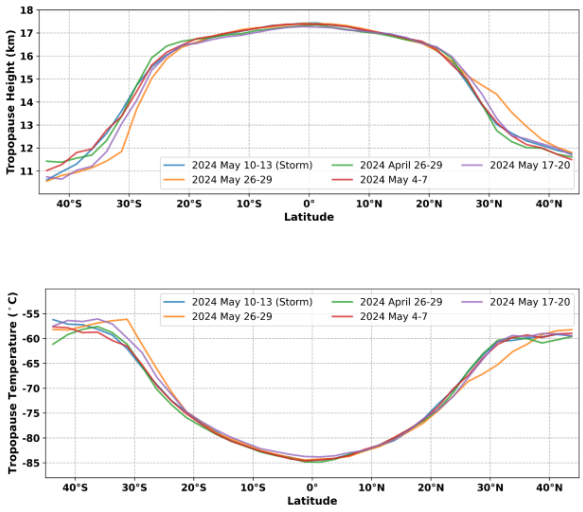

Figure 8: TRH and TRT variation with latitude in period with geomagnetic storm and in period without storm.

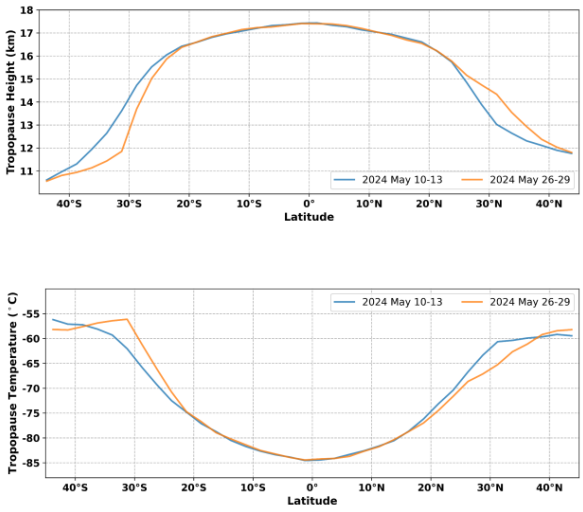

Figure 9: TRH and TRT variation with latitude in period with geomagnetic storm and in period without storm.

Table 1: Parameters obtained from paired t-test at 95% confidence level for the TRH and TRT before, during and after the geomagnetic storm.

Latitude	Before and during storm			During and after storm		
	For TRH		Significance at p<0.05	For TRH		Significance at p<0.05
	t-statistics	p-value		t-statistics	p-value	
0°–23°	-1.593	0.129	No	9.026	<0.001	Yes
23°–35°	0.268	0.794	No	-0.863	0.415	No
>35°	-0.637	0.544	No	-0.124	0.904	No

Latitude	Before and during storm			During and after storm		
	For TRT		Significance at p<0.05	For TRT		Significance at p<0.05
	t-statistics	p-value		t-statistics	p-value	
0°–23°	0.779	0.447	No	-5.994	<0.001	Yes
23°–35°	0.670	0.520	No	2.598	0.288	No
>35°	1.396	0.205	No	13.80	<0.001	Yes

3.3 Discussion

The nature of the global TRH and TRT during the time of the geomagnetic storm from 10-13 May 2024 similar to the global trend as suggested by Rieckh et al. (2014) [23] and Zhren & Mousa (2023) [24]. This indicates that during geomagnetic storm there is no any significant change in shape of the variation of tropopause parameters with latitude.

From yearly comparison of global TRH and TRT, it can be said that the discrepancies observed in the tropical region is due to the effect of global warming [25] as well as the increase in global temperature in 2024, since, May 2024 was the hottest May recorded ever [26]. The differences observed in sub-tropical and high-latitude region is due to the geomagnetic storm. The significant difference observed between TRH and TRT during and after the geomagnetic storm strongly support the coupling between the ionosphere and upper troposphere. The During Geomagnetic storm, large amount of the energy flows from magnetosphere towards the ionosphere at high latitude region. This could produce heating and drag resulting the various types of waves, such as; gravity wave and planetary waves, which can propagate up to the upper part of the troposphere [27,28]. The higher value of the TRH and lower value of TRT in northern hemisphere comparison to southern hemisphere is due to the orientation of the Earth towards the Sun in this season, which causes higher temperature in northern hemisphere compare to southern hemisphere.

4 Conclusions

In this work, we have studied the behavior of the global TRH and TRT in the periphery of the geomagnetic storm time 10-13 May 2024. The result obtained is compared with the days before and after the geomagnetic storm as well as the same day in previous year. Following are the major conclusions;

- The value of global TRH is found almost constant in tropical region (0° to ∼23° latitude) and beyond sub-tropical region (>35°) but decreases sharply in sub-tropical region (∼23°to ∼35° latitude) in both hemisphere in the periphery of May 2024.
- The value of global TRT is increasing slowly with the increase in latitude in the tropical region, but increases sharply in sub-tropical region. Beyond sub-tropical region, TRT remains almost constant in the periphery of May 2024.
- At higher latitude (>35°), the value of TRH us slightly higher and TRT is slightly lower towards northern hemisphere compare to southern hemisphere due to the orientation of the Earth with respect of Sun in this season.
- In comparison to prior years, the TRH is increased even in the equatorial region during the period of geomagnetic storm of May 2024. This seemed to indicate the likely impact of geomagnetic storm on TRH but on further analysis this increase was found to be due to global warming and the global increase in temperature in May 2024.
- There is no significant difference in TRH and TRT before and during the geomagnetic storm in all geographical regions but difference is observed during storm time and quiet time after the storm. Which supports the coupling mechanism between ionosphere and upper atmosphere.

The study of the effect of the geomagnetic storm on the troposphere and tropopause is very important. This study is limited between geomagnetic latitude 45°S to 45°N due to the limitation of COSMIC-2 data. Similar types of study for more geomagnetic storm events at different seasons including higher latitude data is necessary to explore the effects furthermore.

Acknowledgements

The first and corresponding author acknowledge their host institute Department of Physics, Tri-Chandra Multiple Campus, TU and Central Department of Physics, TU, for the all types of academic support in this work. Corresponding author acknowledges UGC for providing PhD fellowship, **UGC award number: PhD – 81/82 – S&T – 17**. Thanks to Taiwan Space Agency and Omni Web Data Explorer for the availability of the data used for this work.

References

[1] K. Mohanakumar. *Stratosphere Troposphere Interactions: An Introduction*. Springer Netherlands, 2008.

[2] W. H. Schlesinger and E. S. Bernhardt. The atmosphere. In *Biogeochemistry*, pages 51–97. 2020.

[3] J. M. Wallace and P. V. Hobbs. *Atmospheric Science: An Introductory Survey*, volume 92. Elsevier, 2006.

[4] J. Lastovicka. Solar wind and high-energy particle effects in the middle atmosphere. In *International Council of Scientific Unions, Middle Atmosphere Program. Handbook for MAP*, volume 29. 1986.

[5] J. Lastovicka. Effects of geomagnetic storms in the lower ionosphere, middle atmosphere and troposphere. *Journal of Atmospheric and Terrestrial Physics*, 58(7):831–843, 1996.

[6] G. S. Lakhina and B. T. Tsurutani. Geomagnetic storms: Historical perspective to modern view. *Geoscience Letter*, 3:1–11, 2016. doi:10.1186/s40562-016-0037-4.

[7] M. Moldwin. *An Introduction to Space Weather*. Cambridge University Press, 2022.

[8] G. P. Petropoulos and P. K. Srivastava. *GPS and GNSS Technology in Geosciences*. Elsevier Science, 2021.

[9] W. S. Schreiner et al. Cosmic-2 radio occultation constellation: First results. *Geophysical Research Letters*, 47(4):e2019GL086841, 2020. doi:10.1029/2019GL086841.

[10] M. Grandin et al. The gannon storm: Citizen science observations during the geomagnetic superstorm of 10 may 2024. *Geoscience Communication*, 7(4):297–316, 2024. doi:10.5194/ge-7-297-2024.

[11] G. Fjeldbo, A. J. Kilore, and V. R. Eshleman. The neutral atmosphere of venus as studied with the mariner v radio occultation experiments. *Astronomical Journal*, 76:123, 1971.

[12] H. Gleisner, M. A. Ringer, and S. B. Healy. Monitoring global climate change using gnss radio occultation. *Npj Climate and Atmospheric Science*, 5(1):6, 2022.

[13] E. R. Kursinski, G. A. Hajj, S. S. Leroy, and B. Herman. The gps radio occultation technique. *Terrestrial Atmospheric Oceanic Science*, 11(1):53–114, 2000.

[14] E. K. Smith and S. Weintraub. The constants in the equation for atmospheric refractive index at radio frequencies. *Proceeding of the IRE*, 41(8):1035–1037, 1953.

[15] World Meteorological Organization. Meteorology - a three-dimensional science: Second session of the commission for aerology. Technical Report Technical Paper No. 45, World Meteorological Organization, Geneva, Switzerland, 1957.

[16] K. Atkinson. *An Introduction to Numerical Analysis*. Wiley, 1991.

[17] M. S. Paudel, B. D. Ghimire, and N. P. Chapagain. Seasonal tropopause dynamics over nepal from 2022 to 2023: Insights from gnss-ro observations. *Journal of Nepal Physical Society*, 10(1):92–100, 2024. doi:10.3126/jnphyssoc.v10i1.73389.

[18] D. J. Seidel and W. J. Randel. Variability and trends in the global tropopause estimated from radiosonde data. *Journal of Geophysical Research: Atmospheres*, 111(D21), 2006. doi:10.1029/2006JD007363.

[19] W. J. Randel, F. Wu, and D. J. Gaffen. Interannual variability of the tropical tropopause derived from radiosonde data and ncep reanalyses. *Journal of Geophysical Research: Atmospheres*, 105(D12):15509–15523, 2000. doi:10.1029/2000JD900155.

[20] S. Fueglistaler, A. E. Dessler, T. J. Dunkerton, I. Folkins, Q. Fu, and P. W. Mote. Tropical tropopause layer. *Reviews of Geophysics*, 47(1), 2009. doi:10.1029/2008RG000267.

[21] Z. Liu, Y. Sun, W. Bai, J. Xia, G. Tan, C. Cheng, and D. Wang. Comparison of ro tropopause height based on different tropopause determination methods. *Advances in Space Research*, 67(2):845–857, 2021. doi:10.5194/amt-2019-379.

[22] T. Rieckh, B. Scherllin-Pirscher, F. Ladstädter, and U. Foelsche. Characteristics of tropopause parameters as observed with gps radio occultation. *Atmospheric Measurement Techniques*, 7(11):3947–3958, 2014. doi:10.5194/amt-7-3947-2014.

[23] E. L. Lehmann and J. P. Romano. *Testing Statistical Hypotheses*. Springer New York, New York, NY, 2005.

[24] M. Zhran and A. Mousa. Global tropopause height determination using gnss radio occultation. *The Egyptian Journal of Remote Sensing and Space Science*, 26(2):317–331, 2023. doi:10.1016/j.ejrs.2023.04.004.

[25] P. Lin, D. Paynter, Y. Ming, and V. Ramaswamy. Changes of the tropical tropopause layer under global warming. *Journal of Climate*, 30(4):1245–1258, 2017. doi:10.1175/JCLI-D-16-0457.1.

[26] National Oceanic and Atmospheric Administration. May 2024 was earth's warmest may on record. https://www.noaa.gov/news/may-2024-was-earths-warmest-may-on-record, 2024. Online article.

[27] A. D. Danilov and J. Lastovicka. Effects of geomagnetic storms on the ionosphere and atmosphere. *International Journal of Geomagnetism and Aeronomy*, 2(3):209–224, 2001.

[28] A. Seppälä, H. Lu, M. A. Clilverd, and C. J. Rodger. Geomagnetic activity signatures in wintertime stratosphere wind, temperature, and wave response. *Journal of Geophysical Research: Atmospheres*, 118(5):2169–2183, 2013. doi:10.1002/jgrd.50236.